ELSEVIER

Journal of Organometallic Chemistry 652 (2002) 95–104

Journal of Organometallic Chemistry

www.elsevier.com/locate/jorganchem

Photochemical intermediates of *trans*-Rh(CO)L_2Cl where L = PMe_3, PBu_3, and *i*-Pr_2HN and *cis*-Rh(CO)$_2$(*i*-Pr_2HN)Cl in frozen organic glasses

Thomas E. Bitterwolf [a,*], W. Bruce Scallorn [a], J. Timothy Bays [a], Callie A. Weiss [a], John C. Linehan [b], James Franz [b], Rinaldo Poli [c]

[a] *Department of Chemistry, University of Idaho, Moscow, ID 83844-2343, USA*
[b] *Chemical Sciences Department, Pacific Northwest National Laboratory, PO Box 999, Richland, WA 99352, USA*
[c] *Laboratoire de Syntheses et d'Electrosynthese Organometalliques, Université de Bourgogne Faculté de Sciences "Gabriel", 21100 Dijon, France*

Received 18 October 2001; received in revised form 31 January 2002; accepted 1 February 2002

Abstract

The Nujol glass matrix photolyses of Rh(CO)(PMe_3)$_2$Cl (**1**), Rh(CO)(PBu_3)$_2$Cl (**2**), Rh(CO)$_2$(*i*-Pr_2HN)Cl (**3**), and Rh(CO)(*i*-Pr_2HN)$_2$Cl (**4**), have been examined. Photolysis of **1** ($\lambda_{irr} > 400$ nm) and **2** ($350 < \lambda_{irr} < 400$ nm) give new species, **A**, with carbonyl stretching bands slightly below the parent bands. In the case of **1** this species appears to give rise to a second product, **C**, upon either extended photolysis or annealing. High-energy photolysis of **1**, **2**, and **4**, result in loss of CO and formation of an IR silent species, RhL_2Cl. In the case of **1** a new carbonyl species, **B**, is observed upon high-energy photolysis or annealing of a matrix containing CO and Rh(PMe_3)$_2$Cl. **B** may be converted to **1** by either back photolysis or annealing. Compound **3** undergoes photochemical CO-loss to form two isomeric photoproducts. Comparison of the carbonyl stretching frequencies of phosphine and ammine derivatives and photoproducts made it possible to eliminate PR_3 loss as the source of **A**. DFT calculations suggest that **A** may be a non-planar, triplet excited state of **1** or **2**. DFT calculations also support the assignment of **B** to *cis*-Rh(CO)(PMe_3)$_2$Cl.

Keywords: Photolysis; Amine derivatives; DFT analysis

1. Introduction

The recent simultaneous publication of photochemical strategies for the carbonylation of ethane [1] and methane [2] using *trans*-Rh(CO)(PMe_3)$_2$Cl in supercritical CO_2 (sc-CO_2) attests to a continuing interest in the utilization of rhodium(I) photocatalysts to carry out fundamental chemical transformations on hydrocarbon substrates. Photoassisted carbonylation of C–H bonds in aromatic hydrocarbons and alkanes has been reported by Fisher and Eisenberg [3], Tanaka and coworkers [4], Browse and Goldman [5] and their coworkers. For benzene, Reaction (1) has been shown to be catalyzed by a number of metal carbonyl phosphine compounds including IrH_3(CO)(dppe) [3a,3c], Ir(CO)(PPh_3)$_2$Cl [3b,3c], Rh(CO)(PPh_3)$_2$Cl [3b,3c], Rh(CO)(PPh_3)$_2$H [3b,3c], Rh(CO)(PMe_3)$_2$Cl [4,5] and $Ru(CO)_4(PPh_3)$ [3d].

$$R-H + CO \rightarrow R-CHO \qquad \text{Reaction (1)}$$

In the absence of CO, *trans*-Rh(CO)(PMe_3)$_2$Cl (**1**), catalyzes the thermodynamically unfavorable dehydration of alkanes. Goldman and coworkers [6] have examined the mechanism of this reaction and developed convincing evidence that the photolysis ($\lambda_{irr} = 366 \pm 20$ nm) results in CO-loss to form [Rh(PMe_3)$_3$Cl], proposed to be the active intermediate in the dehydrogenation process.

Detailed mechanistic studies by Ford and co-workers [7] and Rosini et al. [8] have established that there may be two pathways for these carbonylation reactions. One pathway involves loss of CO forming [Rh(PMe_3)$_2$Cl] that can undergo C–H insertion and subsequent CO

* Corresponding author. Tel.: +1-208-885-6552; fax: +1-208-885-6173.
E-mail address: bitterte@uidaho.edu (T.E. Bitterwolf).

0022-328X/02/$ - see front matter
PII: S0022-328X(02)01312-8

recapture to yield a hexacoordinate species of the general form $Rh(CO)(H)(R)(PMe_3)_2Cl$. A second pathway appears to involve direct reaction of substrate with an excited state of **I** to yield the same intermediate. A secondary photochemical step initiates loss of RCHO from the hexacoordinate intermediate. There is a marked wavelength dependence for the two oxidative addition pathways with CO-loss requiring lower energies. At a photolysis wavelength of 355 nm both pathways appear to be operative although the partitioning between the two pathways is not known.

Tanaka and co-workers [4a,4b] have reported a wavelength dependent product distribution in the photolysis of **1** with toluene and decane. High-energy light ($\lambda_{irr} > 295$ nm) results primarily in *meta* and *para* substitution of toluene and terminal carbonylation of decane. In contrast, lower energy photolysis ($\lambda_{irr} > 375$ nm) results in substantial methyl carbonylation of toluene and internal carbonylation of decane. It is not presently known whether the difference in product distribution is in some way related to the two oxidative addition pathways noted above.

Our long-standing interest in the identification of photochemical intermediates in frozen organic glasses prompted us to initiate what was expected to be a short investigation into the photochemistry of **1**. The results of what ultimately proved to be a multi-year odyssey are reported in this paper.

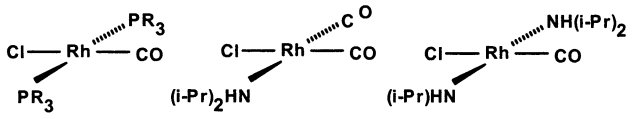

1. R = Me 3 4

2. R = Bu

2. Results

Experimental procedures for photochemical studies in frozen organic glasses have been previously reported [9]. A variety of optical filters were used to control the incident light during photochemical experiments. Compounds **1** [8], *trans*-$Rh(CO)(PBu_3)_2Cl$ (**2**) [10], and *cis*-$Rh(CO)_2(i\text{-}Pr_2HN)Cl$ (**3**) [11], were prepared by standard literature methods. *trans*-$Rh(CO)(i\text{-}Pr_2HN)_2Cl$ (**4**), was prepared by photolysis of **3** in heptane with an excess of $i\text{-}Pr_2HN$. Details of this synthesis will be reported in a subsequent publication [12].

Compound **1** is only moderately soluble in Nujol at room temperature. Samples were prepared by grinding a few crystals of **1** with Nujol followed by lengthy centrifugation to separate fine crystallites. IR spectra of the resulting solutions both at room temperature and at ca. 90 K had single, sharp lines for the carbonyl stretching band of **1** characteristic of Nujol solutions and not the broad bands typical of mulls. Nujol glass solutions of **1** at ca. 90 K are found to have two absorption bands at 360 and 275 nm (Fig. 1). At room temperature these bands are considerably broadened. Neither IR nor UV–vis spectra contained any bands that might be attributed to d–d stacked dimers or oligomers.

Photolysis of Nujol glass solutions of **1** at $\lambda_{irr} > 450$ nm resulted in no detectable changes in the IR spectrum. Photolysis at $\lambda_{irr} = 400 \pm 70$ nm resulted in a decrease in the intensity of the band of **1** at 1964 cm^{-1} and growth of a new band at 1955 cm^{-1}. Upon extended photolysis ($\lambda_{irr} \geq 400$ nm, 6 h) a low, broad band may be discerned at about 1938 cm^{-1} (Fig. 2a). No band for 'free' CO (2131 ± 2 cm^{-1}) is observed at these photolysis wavelengths even after very long photolyses. Annealing a sample photolyzed in this manner to 153 K resulted in decrease of the 1955 cm^{-1} band, growth of the band at 1964 cm^{-1} and small growth in the band at 1938 cm^{-1} (Fig. 2b).

Photolysis of a fresh sample of **1** ($330 < \lambda_{irr} < 400$ nm, 1 h) results in a decrease in the carbonyl band of **1** and growth of bands at 2131, 2012, 1954, and 1938 cm^{-1} (Fig. 3a). Photolysis of a fresh sample of **1** ($\lambda_{irr} = 280 \pm 10$ nm, 30 min) resulted in decrease in the band of **1** and growth of bands at 2131 and 2012 cm^{-1} (Fig. 4a). Back photolysis of this sample ($\lambda_{irr} = 450 \pm 70$ nm, 10 min) resulted in a bleaching of the band at 2012 cm^{-1} and growth of a band at 1962 cm^{-1} presumed to be **1**, with a low energy shoulder at 1955 cm^{-1} (Fig. 4b). The band at 1955 cm^{-1} may be a result of direct photolysis of **1** at this wavelength and not be related to the back photolysis of the 2012 cm^{-1} band.

Annealing studies of a sample of **1** that had been photolyzed for an extended time ($\lambda_{irr} = 280 \pm 10$ nm, 4.5 h) were particularly informative. As before, photolysis resulted in a decrease in the band of **1** and growth of bands at 2131 and 2012 cm^{-1} (Fig. 5a). Annealing this sample to 130 K resulted in a decrease in the band at 2131 and a previously unseen band at 1955 cm^{-1} and

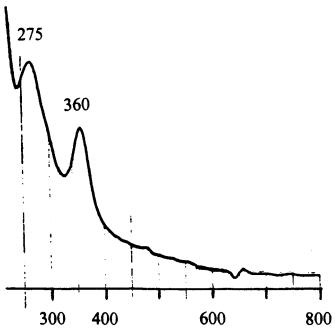

Fig. 1. Electronic spectrum of **1** in Nujol at ca. 90 K. The small features at 475 and 650 nm are instrument artifacts.

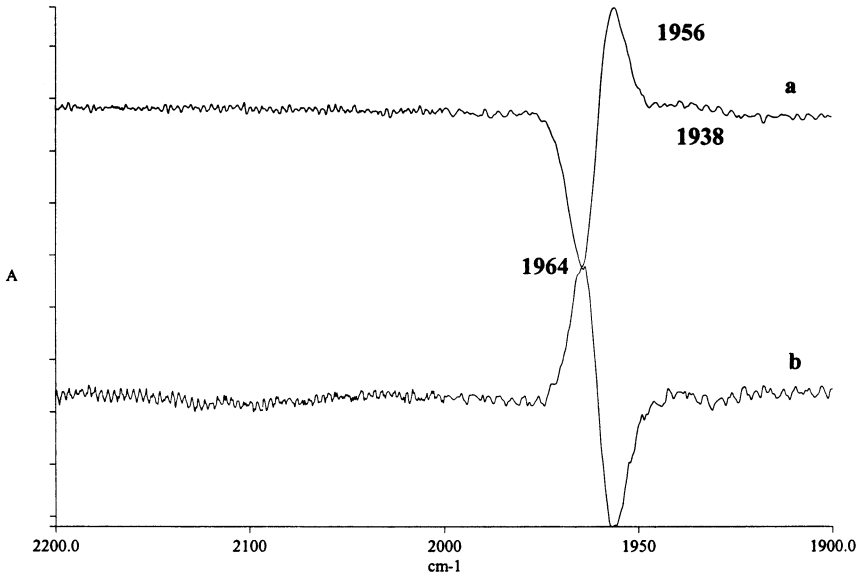

Fig. 2. (a) 6 h photolysis of **1**, $\lambda_{irr} > 400$ nm. (b) Anneal of sample to 153 K.

growth of bands at 2012, 1964, and 1938 cm^{-1} (Fig. 5b). Further annealing to 170 K resulted in further decrease in the bands at 2131 and 1955 cm^{-1} as well as a decrease in the band at 2012 cm^{-1} and growth of the bands at 1964 and 1938 cm^{-1} (Fig. 5c).

To clarify the identity of the new species, ^{13}CO labeled **1** (about 90% enrichment that also contains a trace of $^{13}C^{18}O$) was prepared and photolyzed ($330 < \lambda_{irr} < 400$ nm, 15 min) (Fig. 3b). Bands of **1** (1962 cm^{-1}), **1**-^{13}CO (1916 cm^{-1}), and **1**-$^{13}C^{18}O$ (1873 cm^{-1}) were found to decrease while new bands at 2082, 2011, 1968, 1954, 1908, and 1865 cm^{-1} were found to grow in. The observed bands at 1908 and 1865 cm^{-1} correspond to the ^{13}CO and $^{13}C^{18}O$ labeled analogues of the species at 1955 cm^{-1}, while the band at 1968 cm^{-1} corresponds to the ^{13}CO labeled analogue of the previously observed band at 2012 cm^{-1}. The band at 2082 cm^{-1} is 'free' ^{13}CO in the Nujol glass matrix. Free ^{12}CO and $^{13}C^{18}O$ were not detectable above the background noise.

In 2-methyltetrahydrofuran glass at ca. 90 K, **1** has a slightly broadened band at 1961 cm^{-1}. Photolysis of this band at energies as low as 500 nm resulted in a decrease in the bands of **1** and growth of a band at 1952 cm^{-1}. Higher energy photolysis resulted in CO loss, but no new bands were observed.

Photolysis ($350 < \lambda_{irr} < 400$ nm, 30 min) of a frozen Nujol glass sample of **2** resulted in a decrease in the band of **2** (1954 cm^{-1}) and growth of a new band at

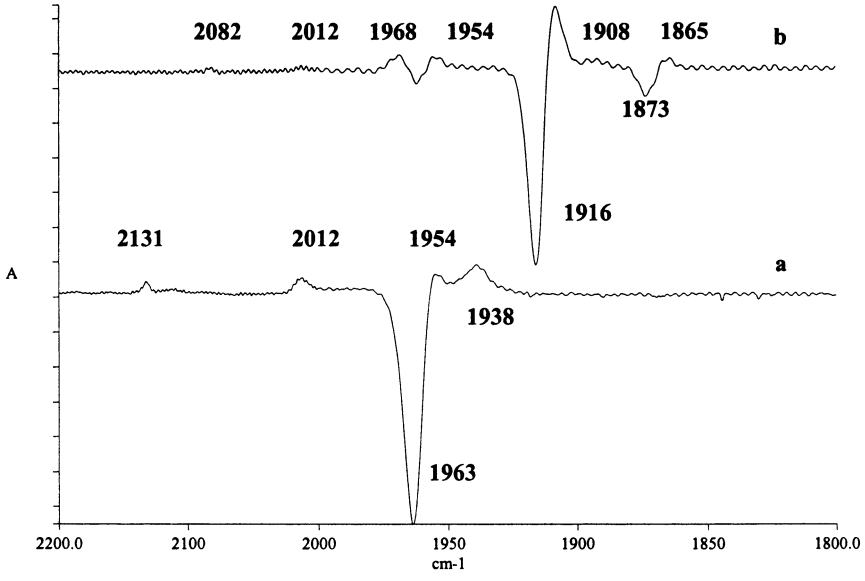

Fig. 3. (a) 1 h photolysis of **1**, $330 < \lambda_{irr} < 400$ nm. (b) 15 min photolysis of ^{13}CO labeled **1**, $330 < \lambda_{irr} < 400$ nm.

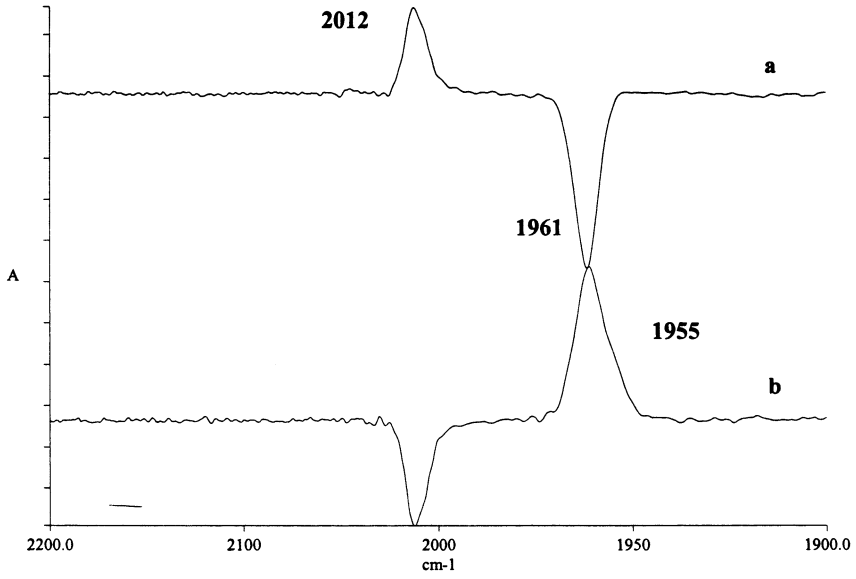

Fig. 4. (a) 30 min photolysis of **1**, $\lambda_{irr} = 280 \pm 10$ nm. (b) 10 min back photolysis, $\lambda_{irr} = 450 \pm 70$ nm.

1947 cm^{-1}. No free CO was observed under these conditions. Further photolysis of this sample ($330 < \lambda_{irr} < 400$ nm, 30 min) resulted in a substantial bleaching of the band of **2** and appearance of a band at 2130 cm^{-1}. No other product bands were observed.

Photolysis of **3** in frozen Nujol at $\lambda_{irr} > 400$ nm resulted in no apparent change in the IR spectral bands of **3** at 2080 and 2000 cm^{-1}. Photolysis ($330 < \lambda_{irr} < 400$ nm, 15 min) resulted in a decrease in the bands of **3** and growth of bands at 2131, 1977, and 1960 cm^{-1} (Fig. 6).

Photolysis of a sample of **4** containing a trace of **3** in frozen Nujol at $\lambda_{irr} > 400$ nm exhibited no apparent change. Higher energy photolysis ($330 < \lambda_{irr} < 400$ nm, 15 min) resulted in a decrease in the band of **4** and the appearance of a new band at 2131 cm^{-1}. No other spectral features attributable to photoproducts of **4** were observed.

Summarizing our photochemical observations, low energy photolysis of both **1** and **2** result in the appearance of a new species, **A**, with IR bands slightly below those of the parent species. No such photoproduct was observed in the photolysis of the bis(ammine) derivative **4**. Medium energy photolysis, $330 < \lambda < 400$ nm, of **1**, **2**, and **4** result in loss of CO to yield an IR silent photoproduct presumed to be RhL_2Cl. In addition, a new species with a carbonyl band at 2012 cm^{-1}, **B**, is observed to form in both the medium and the high energy photolysis of **1**. Interestingly at the highest

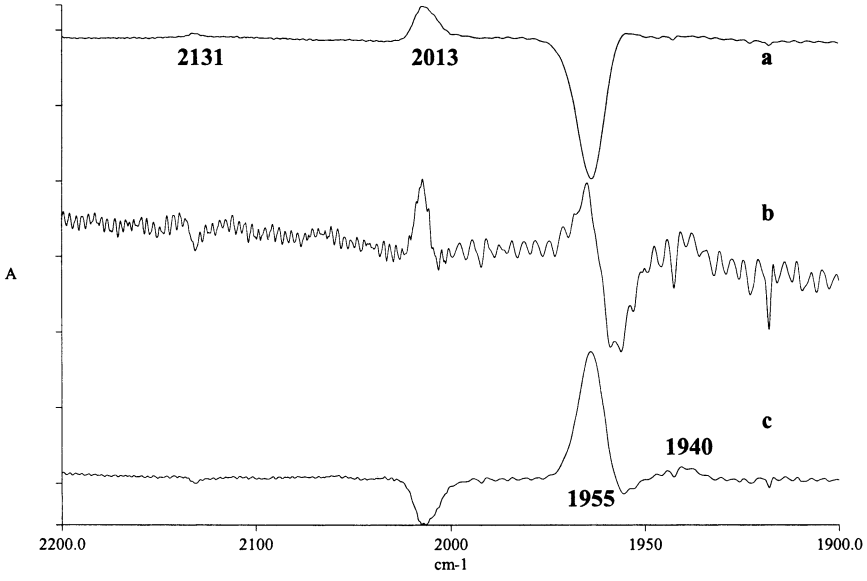

Fig. 5. (a) 4.5 h photolysis of **1**, $\lambda_{irr} = 280 \pm 10$ nm. (b) Anneal to 130 K. (c) Anneal to 170 K.

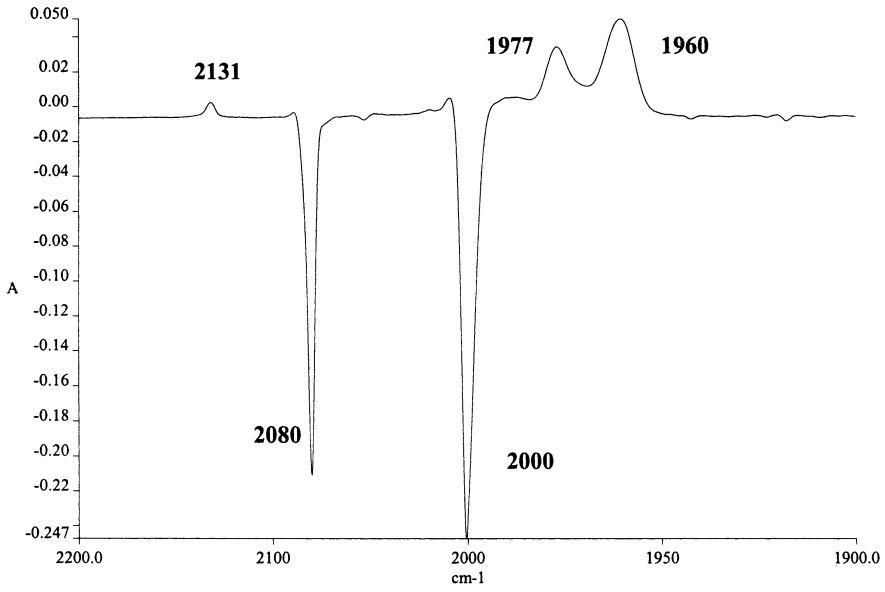

Fig. 6. 15 min photolysis of **3**, $330 < \lambda_{irr} < 400$ nm.

energies investigated, $\lambda = 280 \pm 10$ nm, **B** appears to be the dominant product with relatively no CO loss as evidenced by the small bands at 2131 cm^{-1}. **B** also appears upon annealing of matrices that have been photolyzed at high energy and thus contain free CO. **B** is converted to **1** by either annealing or long wavelength back photolysis. Finally, a species with an IR band at 1938 cm^{-1}, **C**, appears on extended, low energy photolysis of **1** or upon annealing of matrices containing **A**. At long wavelength irradiation relatively little **C** is formed, but the relative amounts of this species increase with photolysis in the near UV. Interestingly, photolysis at 280 nm yields very little of either **A** or **C**. No bands comparable to **B** or **C** were observed in the photolysis of **2**. Photolysis of the mono(ammine) derivative, **3**, results in loss of CO and appearance of two new carbonyl bands.

In an effort to clarify the identities of the various species present in the photolysis of **1** an effort was made to prepare and isolate *cis*-$Rh(CO)_2(PMe_3)Cl$. Trimethylphosphine was slowly added to a solution of $Rh_2(CO)_4Cl_2$ in petroleum ether under CO as described by Poliblanc and co-workers [13] with the formation of $Rh(CO)_2(PMe_3)Cl$ being confirmed by the appearance of carbonyl bands at 2093 and 2001 cm^{-1}. A CO saturated solution was stored at -78 °C for several days during which time cherry red crystals appeared. All attempts to isolate these crystals resulted in a rapid color change from bright red to dull tan. The resulting tan product was shown by IR to be $Rh_2(CO)_2(PMe_3)_2(\mu\text{-}Cl)_2$. We believe that the red crystals are $Rh(CO)_2(PMe_3)Cl$ and attribute their color to the well known d–d stacking effects observed for some $Rh(CO)_2$(ammine)Cl derivatives [11,14]. When petroleum ether solutions containing $Rh(CO)_2(PMe_3)Cl$ were frozen to liquid nitrogen temperatures a purple color was observed that we believe to be due to continued growth of d–d stacks at low temperature.

3. Discussion

The lowest energy photoproduct, **A**, of **1** and **2** forms upon photolysis into the bottom edge of the 360 nm band without loss of CO. In our preliminary analysis of these spectra we speculated that it might arise from loss of a PMe_3 ligand as has been reported by Perutz and coworkers [15] for *cis*-$Ru(PMe_3)_4H_2$. Reinforcing this hypothesis was the similarity of the IR band of $[Rh(CO)(PMe_3)_3]Cl$ with that of **C**.

Our attempts to prepare and isolate $Rh(CO)_2(PMe_3)Cl$ as a precursor to the putative $[Rh(CO)(PMe_3)Cl]$ intermediate proved unsuccessful, thus we opted to prepare a corresponding ammine series of derivatives to serve as analogues. The choice of ammine in this case was dictated by our desire for a comparatively simple ligand, but also one that would preclude d–d stacking of the square-planar rhodium molecules. Our first choice for a model compound was the previously unknown $Rh(CO)_2(Et_3N)Cl$. While this compound was easily formed upon addition of Et_3N to $Rh_2(CO)_4(\mu\text{-}Cl)_2$, it proved to be exceptionally air-sensitive giving rise to a blue species, we believe to be an O_2 adduct. It appears that there has only been one other report of an attempted synthesis of $Rh(CO)_2LCl$ derivatives with tertiary amines and these compounds were simply described as being unstable [16]. Although we were ultimately able to carry out Nujol matrix studies on $Rh(CO)_2(NEt_3)Cl$ that parallel the results for the di(isopropyl)amine derivative described below,

the quality of these spectra were not high and it was clear that impurities were present.

As an alternative to $Rh(CO)_2(Et_3N)Cl$, the known, air-stable derivative $Rh(CO)_2(i\text{-}Pr_2HN)Cl$ (**3**), was prepared. Compound **3** is known to exist in the solid state and in solution as a monomeric species [11]. IR bands of **3** are observed in Nujol at 2080 and 2000 cm^{-1}, somewhat lower in energy than $Rh(CO)_2(PMe_3)Cl$ in CO saturated petroleum ether for which bands are observed at 2094 and 2001 cm^{-1}.

Photolysis of **3** is expected to give rise to two isomeric carbonyl loss products (Fig. 7) as is observed. Chloride is a potential π-electron donor while there can be no comparable donation from the ammine ligand. Accordingly, we have assigned the photoproduct with the lower carbonyl stretching frequency (1960 cm^{-1}) to the isomer with the carbonyl *trans* to the chloride, and the species with the higher carbonyl stretching frequency (1977 cm^{-1}) to the isomer with the carbonyl *trans* to the ammine.

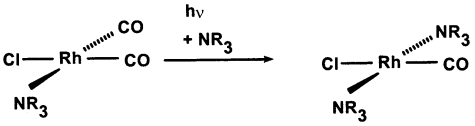

Reaction(2)

Photolysis of **3** in heptane with an excess of di(isopropyl)amine resulted in formation of **4** along with a dark decomposition product, Reaction (2). The carbonyl stretching band of **4** is found at 1940 cm^{-1} in Nujol while the comparable band of **1** appears at 1962 cm^{-1}. The differences in carbonyl stretching frequencies are readily explained by the difference in π-acidic character of the two ligands. The ammine has no π-acidic character thus backbonding transfers more metal electron density to the carbonyl ligand in the ammine derivative than in the phosphine case. Matrix photolysis of **4** indicates that CO is lost at high energy, but there are no other intermediates analogous to those observed for **1** or **2**. We are presently exploring the solution photochemistry of **4** and other bis(ammine) derivatives.

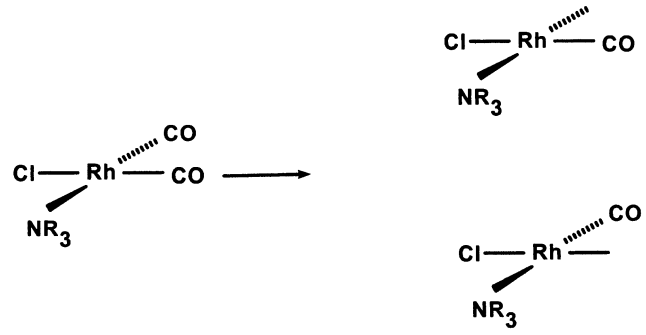

Fig. 7. CO-loss isomeric photoproducts of $Rh(CO)_2$(ammine)Cl derivatives.

By analogy with the carbonyl stretching frequencies of **1** and **4** we would anticipate the putative PMe_3-loss intermediate $[Rh(CO)(PMe_3)Cl]$ to have a carbonyl stretching frequency ca. 22 cm^{-1} above that of its ammine analogue (1960 cm^{-1}) or about 20 cm^{-1} above that of **1**. DFT calculations on **1** and $[Rh(CO)(PMe_3)Cl]$ predict the monophosphine species to have a carbonyl stretching frequency 29 cm^{-1} above that of **1**. This is remarkably consistent with our prediction above. We note that $[Rh(CO)(i\text{-}Pr_2HN)Cl]$ has a carbonyl stretching frequency 20 cm^{-1} above that of $Rh(CO)(i\text{-}Pr_2HN)_2Cl$. These data are summarized in Fig. 8. Based on this analysis, we must conclude that the photoproduct **A** cannot be assigned to the phosphine loss species $[Rh(CO)(PMe_3)Cl]$.

Brady et al. have reported electronic spectral studies on a series of square-planar complexes of the form $M(CO)L_2Cl$, where M = Rh and Ir, and L = PR_3, where R = alkyl and aryl groups [17]. It was noted that electronic transitions at 360 nm sharpened when observed at 77 K, but the reported measurements did not extend below 300 nm, thus the 275 nm feature observed in the current work was not seen. Brady et al. attribute the 360 nm transition to an $a_1(z^2)$–$b_1\pi$ (HOMO–LUMO) transition with MLCT character. The second highest excitation would be $a_1(z^2)$–$a_1(x^2-y^2)$. Since the latter orbital is antibonding with respect to the ligands it may well be associated with the higher energy CO-loss excitation. The electronic spectra of the C_{2v} $M(CO)L_2Cl$ species parallel to those observed for D_{4h} $[M(PC_2P)_2]^{+1}$ and $[M(PC{=}CP)_2]^{+1}$ complexes and are typically interpreted by analogy to the more symmetric case (Fig. 9). Geoffroy et al. [18] and Fordyce and Crosby [19] have noted that the lower energy transition of the complexes with D_{4h} symmetry is $^1A_{1g}$–$^3A_{2u}$ (a_{1g}–a_{2u}), while the next higher energy band is $^1A_{1g}$–$^1A_{2u}$ (a_{1g}–a_{2u}). It is interesting to note that large Stokes shifts observed in the emission spectra of Rh(I) D_{4h} complexes have been interpreted to suggest substantial distortion of the

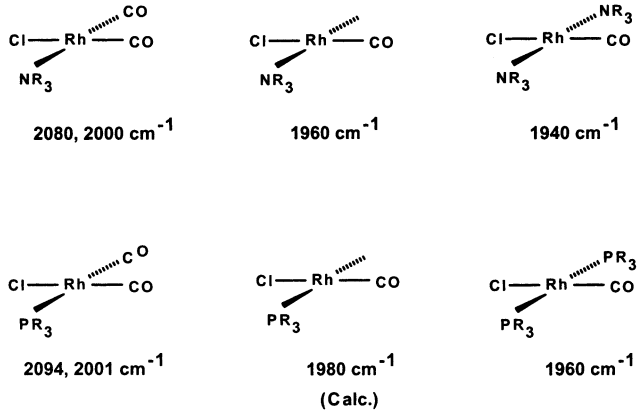

Fig. 8. Summary of observed and calculated rhodium carbonyl phosphine and ammine derivatives.

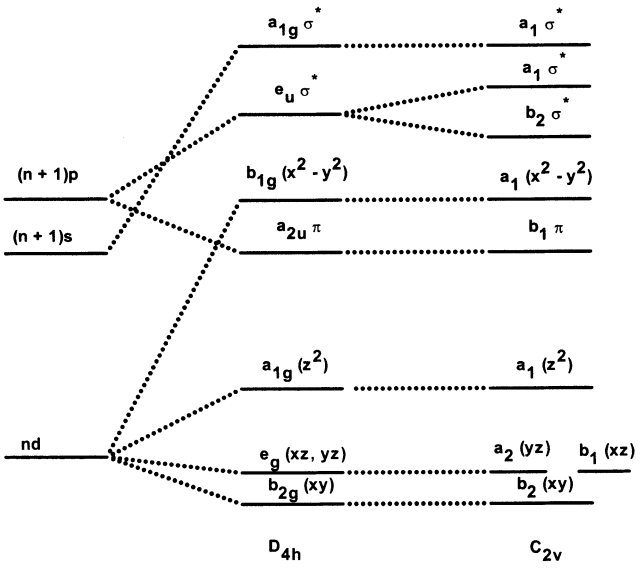

Fig. 9. Molecular orbital energy level diagram (ref. [17]).

excited states. Geoffroy et al. [18] propose that the emitting state is not purely MLCT in character, but includes one or more d–d states leading to a tetrahedral distortion. We shall return to this point below.

As noted above, spectral studies on Rh(I) complexes have suggested that the lowest energy electronic transition is consistent with a triplet excited state, and that some evidence exists to suggest that this excited state deviates from square-planar geometry. We have carried out density functional theory (DFT) calculations of **1** and its PH_3 model compound in an attempt to better understand the nature of this excited state. Calculated bond lengths and angles for $Rh(CO)(PH_3)_2Cl$ and **1** are presented in Tables 1 and 2 along with crystallographically derived values for **1**. The calculated structures are presented in Fig. 10. Calculated energies and CO stretching frequencies are presented in Table 3.

$Rh(CO)(PH_3)_2Cl$ was found to have two excited state, triplet geometries: a distorted-planar geometry that lies 36.4 kcal mol^{-1} above the ground state and a non-planar geometry in which the chloride ligand has moved out of the molecular plane that is 30.8 kcal mol^{-1} above the ground state. The geometries of these triplet species are presented in Fig. 10. These very surprising results prompted us to carry out calculations on **1** itself, for which we found a non-planar triplet excited state 35.3 kcal mol^{-1} above the ground state. Like the PH_3 case, the chloride ligand was found to have moved out of the molecular plane. Bond lengths and angles of the three triplet species are given in Table 1. Calculations of the IR frequencies of both the ground and excited states were carried out and these values are presented in Table 3. The calculated ground state vibrational frequency is 1912 cm^{-1} and the frequency of the triplet species is calculated to be about 1.5 cm^{-1} below this. DFT calculated absolute values of vibrational frequencies for metal complexes are often observed to be shifted to lower energy and calculations on excited state species are particularly difficult. For this reason we note that calculations lend cautious support to the assignment of the species observed at 1955 cm^{-1} to a non-square-planar triplet which is stabilized by the low temperatures and relatively inert matrix. This is consistent with the ease of conversion of this species to the starting material upon annealing.

Table 1
Calculated bond lengths (Å) and angles (°) for $Rh(CO)(PH_3)_2Cl$

	Singlet	Triplet, non-planar	Triplet, planar
Bond lengths			
Rh–P	2.393	2.537	2.735
Rh–Cl	2.447	2.515	2.514
Rh–C	1.842	1.925	1.935
C–O	1.187	1.181	1.179
Bond angles			
Cl–Rh–P	84.59	86.74	79.13
Cl–Rh–C	180.00	108.61	179.98
P–Rh–P	169.18	153.60	158.25
P–Rh–C	95.42	103.16	100.87
Rh–C–O	179.98	175.71	180.00

The data from both photolysis and annealing experiments suggest that **C** either arises as a secondary photolysis product of **A** or through warming of **A**. **C** is unaffected by annealing to as high as 170 K. The identity of this species is an enigma to us as an oxidative addition reaction between the metal and Nujol or a PMe_3 ligand would yield a Rh(III) species that should exhibit higher carbonyl frequencies, not lower frequencies. The dilution of **1** in the Nujol matrices is sufficiently high as such we do not believe that intermolecular interactions between rhodium molecules can account for the observed bands.

High energy photolysis of **1** gives rise to CO-loss as well as to the appearance of a new species, **B**, with a carbonyl band at 2012 cm^{-1}. **B** is transformed to **1** by back photolysis. It is significant that **B** also appears upon annealing of a matrix that had been photolyzed at high energy and thus contained both free CO and the IR silent $Rh(PMe_3)_2Cl$ species. No such species is observed for **2** or for **4**.

Recapture of a CO by $Rh(PMe_3)_2Cl$ results in reformation of **1**, but could also give rise to the *cis* isomer of this compound. The *cis* isomer would be expected to be thermally and photochemically unstable and revert to the *trans* isomer as is observed. Failure to observe comparable bands in the photolysis of **2** may be due to the steric bulk of the tributylphosphine ligands making a *cis* isomer highly unstable. At very high energies it appears that **B** can form directly from **1**, possibly through a tetrahedral excited state.

Table 2
Calculated and experimental bond lengths (Å) and angles (°) for **1**, its non-planar triplet, *cis* isomer and PMe_3 loss species, $Rh(CO)(PMe_3)Cl$

	1, cal.	**1**, exp Ref. [26]	Non-planar triplet	*cis*-$Rh(CO)$-$(PMe_3)_2Cl$	$Rh(CO)(PMe_3)Cl$
Bond lengths					
Rh–P	2.412	2.308	2.512	2.38 (*cis*-CO) 2.498 (*trans*-CO)	2.3887
Rh–Cl	2.471	2.354	2.556	2.4588	2.3887
Rh–C	1.829	1.770	1.920	1.8592	1.8444
C–O	1.191	1.146	1.185	1.1822	1.1876
Bond angles					
Cl–Rh–P	85.66	88.7	87.30	180.03	
Cl–Rh–C	179.98	179.4	106.28	87.59	177.63
P–Rh–P	171.31	177.2	155.21	97.90	
P–Rh–C	94.34	91.3	102.37	180.04 (*trans*) 92.14 (*cis*)	
Rh–C–O	179.97	178.4	179.51	179.56	179.49

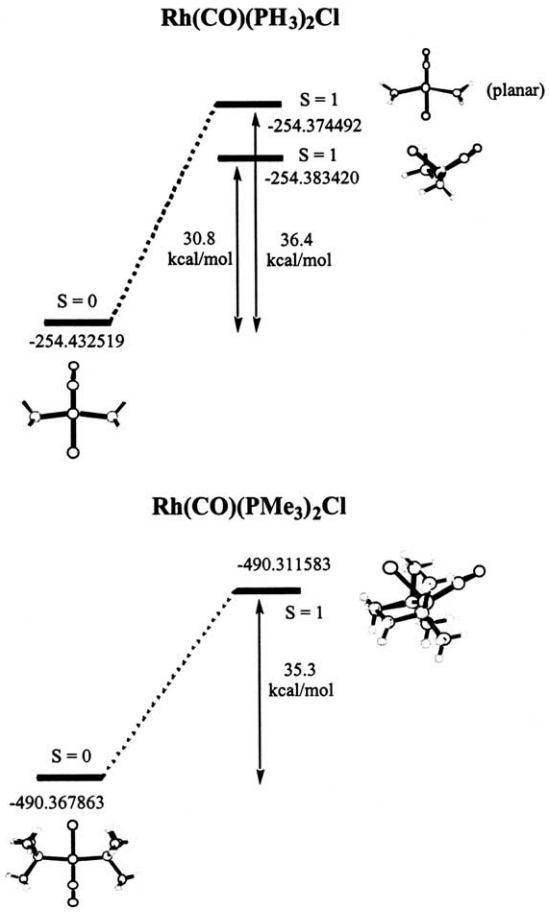

Fig. 10. Computed geometries and energies for $Rh(CO)(PH_3)_2Cl$, $Rh(CO)(PMe_3)_2Cl$ and their related planar and non-planar triplet excited states.

As noted in Section 1, Ford and co-workers [7a] has used time-resolved IR to study the photolysis of **1** in benzene. Two bands observed at 2130 and 2018 cm^{-1} in C_6H_6 were assigned to metal hydride bands. These bands were absent when the photolyses were carried out in C_6D_6. We suggest that the band observed at 2130 cm^{-1} may be attributable to free CO and it is likely that the 2018 cm^{-1} band is due to the same photoproduct observed in these matrix studies. Indeed, we have observed a species at 2019 cm^{-1} in a time-resolved IR study, the photolysis of **1** in supercritical CO_2 [20]. The band at 2019 cm^{-1} decays slightly within the 150 μs time frame of the experiment. We must regard these interpretations as preliminary as we have no explanation for why these bands were not observed in the deuterated solvent.

To further clarify the identity of the 2012 cm^{-1} species we have carried out DFT calculations on *cis*-$Rh(CO)(PMe_3)_2Cl$ and found that this isomer is expected to have a carbonyl stretching frequency 41 cm^{-1} higher than that of the *trans* isomer. This yields a predicted value of 2003 cm^{-1} that is in good agreement with the observed values of 2012–2018 cm^{-1}. Representative calculated bond lengths and angles for the *cis* isomer are presented in Table 2. The difference in carbonyl stretching frequency between the *cis* and *trans* isomers may be readily attributed to the carbonyl group being *trans* to a π-donor chloride in **1** and *trans* to a weak π-acid trimethylphosphine in the *cis* isomer.

4. Conclusions

Solution photochemical studies of **1** by Ford and co-workers [7] and Rosini et al. [8] have provided evidence for the existence of two photochemical pathways in the oxidative addition of hydrocarbons, one involving CO loss and a second involving direct interaction of an excited state of **1** with hydrocarbon. Our matrix studies now provide support for the existence of three distinct photochemical processes: (a) serendipitous observation of a low energy excited triplet, or perhaps a rearranged and stabilized isomer of this species, (b) CO-loss, and (c) direct, high energy formation of the *cis*-$Rh(CO)(PMe_3)_2Cl$ isomer. The *cis*-$Rh(CO)(PMe_3)_2Cl$ isomer may also be formed by recapture of CO by $Rh(PMe_3)_2Cl$. The identity of a further species that

Table 3
Relative energies and calculated CO stretching frequencies for rhodium species

	R = H		R = CH_3		
	E (kcal mol^{-1})	νCO (cm^{-1})	E (kcal mol^{-1})	νCO (cm^{-1}) (cal)	νCO (cm^{-1}) (obs)
$Rh(CO)(PR_3)_2Cl$, singlet	0	1939.06	0	1911.95	1962
$Rh(CO)(PR_3)_2Cl$, Triplet, planar	36.4	1955.73			
$Rh(CO)(PR_3)_2Cl$, Triplet, non-planar	30.8	1937.59	35.3	1910.58	1955
cis-$Rh(CO)(PR_3)_2Cl$			13.7	1952.1	2012
$Rh(CO)(PR_3)Cl$			35.66	1930.2	

appears to be formed from the low energy photointermediate remains unknown.

Finally, it is important to note that the energy range necessary for direct *trans* to *cis* conversion of **1** corresponds to that described by Rosini et al. [8] as being associated with oxidative addition of benzene to the intact excited state of **1**. In both cases these processes would appear to be triggered by photolysis into the electronic band with a maxima at 275 nm.

5. Experimental

Compounds **1** [8], **2** [10], and **3** [11] were prepared by standard literature procedures. The details of the preparation of **4** and other bis(ammine) derivatives will be presented elsewhere [12]. Electronic spectra were recorded on a Cary 2200 Spectrometer. IR spectra were recorded using a Perkin–Elmer Spectrum 1000 FTIR Spectrometer. IR spectra were recorded at 4 cm^{-1} resolution. Nujol matrix studies were carried out using a cryostat designed by Dr. A. Rest of the University of Southampton. 2-Methyltetrahydrofuran matrix studies were carried out using a Graseby Specac Variable Temperature Cryostat. Photolyses were carried out using a 350 W high pressure Hg lamp. Optical filters were used to control the wavelength ranges of the incident radiation.

6. Computational details

All systems have been studied using the B3LYP hybrid density functional theory [21], which has proven to be very reliable for a broad range of organometallic systems similar to those reported here [22]. All geometry optimizations and frequency calculations were carried out with the GAUSSIAN 98 program package [23] using the standard LanL2DZ basis set, which includes both Dunning and Hay's D95 sets for H and C [24] and the relativistic core potential sets of Hay and Wadt for the heavy atoms [25]. The input geometry for the singlet *trans*-$Rh(CO)(PH_3)_2Cl$ and *trans*-$Rh(CO)(PMe_3)_2Cl$ molecules were adapted from the published X-ray structure of the PMe_3 complex [26]. The corresponding triplet structures were obtained starting from a pseudo-tetrahedral input geometry with bond distances set to those obtained from the corresponding singlet optimization. A different, higher energy local minimum having a planar geometry was obtained for the PH3 model compound when starting from the optimized planar geometry of the singlet state. For the larger PMe_3 molecule, this calculation was not carried out. All calculations were carried out without imposed symmetry. Spin contamination was carefully monitored and the value of $\langle S2 \rangle$ for the unrestricted B3LYP calculations on the triplet states at convergence [2.0076 for $RhCl(CO)(PH_3)_2$; 2.0083 for $RhCl(CO)(PMe_3)_2$] indicated minor spin contamination. The energies reported in Sections 2 and 3 do not include a correction for zero-point energy.

Acknowledgements

T.E. B. wishes to thank the Research Corporation for their generous award of a Research Opportunity grant and the Pacific Northwest National Laboratory for financial support. We thank Professor Goldman for his generous gift of our first samples of **1**, and Dr. G. Rosini, Professor Goldman and Professor Ford for helpful advice. We sincerely thank a referee for pointing out the probable direct formation of **B** from **1** at high energy.

References

[1] T.E. Bitterwolf, D.L. Kline, J.C. Linehan, C.R. Yonker, R.S. Addleman, Angewandte Chemie 113 (2001) 2764.
[2] J.-C. Choi, Y. Kobayashi, T. Sakakura, J. Organic Chem. 66 (2001) 5262.
[3] (a) B.J. Fisher, R. Eisenberg, Organometallics 2 (1983) 764;
(b) A.J. Kunin, R. Eisenberg, J. Am. Chem. Soc. 108 (1986) 535;
(c) A.J. Kinin, R. Eisenberg, Organometallics 7 (1988) 2124;
(d) E.M. Gordon, R. Eisenberg, J. Mol. Catal. 45 (1988) 57.
[4] (a) T. Sakakura, T. Sodeyama, K. Sasaki, K. Wada, M. Tanaka, J. Am. Chem. Soc. 112 (1990) 721;
(b) M. Tanaka, T. Sakakura, Pure Appl. Chem. 62 (1990) 1147;
(c) T. Sakakura, K. Sasaki, Y. Tokunaga, K. Wada, M. Tanaka,

Chem. Lett. (1988) 155;
(d) T. Sakakura, M. Tanaka, J. Chem. Soc. Chem. Commun. (1987) 758;
(e) T. Sakakura, M. Tanaka, Chem. Lett. (1987) 1113;
(f) T. Sakakura, M. Tanaka, Chem. Lett. (1987) 249.
[5] W.T. Bowse, A.S. Goldman, J. Am. Chem. Soc. 114 (1992) 350.
[6] (a) G.P. Rosini, S. Soubra, M. Vixamar, S. Wang, A.S. Goldman, J. Organometal. Chem. 554 (1998) 41;
(b) J.A. Maguire, W.T. Boese, A.S. Goldman, J. Am. Chem. Soc. 111 (1989) 7088;
(c) J.A. Maguire, A.S. Goldman, J. Am. Chem. Soc. 113 (1991) 6706.
[7] (a) J.S. Bridgewater, B. Lee, S. Bernhard, J.R. Schoonover, P.C. Ford, Organometallics 16 (1997) 5592;
(b) C.T. Spillett, P.C. Ford, J. Am. Chem. Soc. 111 (1989) 1932;
(c) D.A. Wink, P.C. Ford, J. Am. Chem. Soc. 109 (1987) 436;
(d) D. Wink, P.C. Ford, J. Am. Chem. Soc. 107 (1985) 1794.
[8] G.P. Rosini, W.T. Boese, A.S. Goldman, J. Am. Chem. Soc. 116 (1994) 9498.
[9] (a) T.E. Bitterwolf, K.A. Lott, A.J. Rest, J. Mascetti, J. Organomet. Chem. 419 (1991) 113;
(b) R.H. Hooker, A.J. Rest, J. Chem. Soc. Dalton Trans. (1984) 761.
[10] R.F. Heck, J. Am. Chem. Soc. 86 (1964) 2796.
[11] (a) L.M. Vallarino, S.W. Sheargold, Inorg. Chim. Acta 36 (1979) 243;
(b) D.N. Lawson, G. Wilkinson, J. Chem. Soc. (1965) 1900.
[12] T.E. Bitterwolf, manuscript in preparation, 2001.
[13] (a) E. Rotondo, G. Battaglia, G. Giordano, F.P. Cusmano, J. Organomet. Chem. 450 (1993) 245;
(b) R. Poliblanc, J. Organomet. Chem. 94 (1975) 241;
(c) J. Gallay, D. De Montauzon, R. Poliblanc, J. Organomet. Chem. 38 (1972) 179.
[14] (a) M.C. Torralba, M. Cano, J.A. Campo, J.V. Heras, E. Pinilla, M.R. Torres, J. Organomet. Chem. 633 (2001) 91;
(b) T.W. Thomas, A.E. Underhill, J. Chem. Soc. Rev. 1 (1972) 99.
[15] V. Montiel-Palma, R.N. Perutz, M.W. George, O.S. Jina, S. Sabo-Etienne, J. Chem. Soc. Chem. Commun. (2000) 1175.
[16] M.E. Krafft, L.J. Wilson, K.D. Onan, Organometallics 7 (1988) 2528.
[17] R. Brady, B.R. Flynn, G.L. Geoffroy, H.B. Gray, J. Peone, Jr., L. Vaska, Inorg. Chem. 15 (1976) 1485.
[18] G.L. Geoffroy, M.S. Wrighton, G.S. Hammond, H.B. Gray, J. Am. Chem. Soc. 96 (1975) 3105.
[19] W.A. Fordyce, G.A. Crosby, Inorg. Chem. 21 (1982) 1455.
[20] T.E. Bitterwolf, D.L. Kline, J.C. Linehan, C.R. Yonker, R.S. Addleman, manuscript in preparation, 2002.
[21] A.D. Becke, J. Chem. Phys. 98 (1993) 5648.
[22] S. Niu, M.B. Hall, Chem. Rev. 100 (2000) 353.
[23] M.J. Frisch, G.W. Trucks, H.B. Schlegel, G.E. Scuseria, M.A. Robb, J.R. Cheeseman, V.G. Zakrzewski, J. Montgomery, J.A., R.E. Stratmann, J.C. Burant, S. Dapprich, J.M. Millam, A.D. Daniels, K.N. Kudin, M.C. Strain, O. Farkas, J. Tomasi, V. Barone, M. Cossi, R. Cammi, B. Mennucci, C. Pomelli, C. Adamo, S. Clifford, J. Ochterski, G.A. Petersson, P.Y. Ayala, Q. Cui, K. Morokuma, D.K. Malick, A.D. Rabuck, K. Raghavachari, J.B. Foresman, J. Cioslowski, J.V. Ortiz, A.G. Baboul, B.B. Stefanov, G. Liu, A. Liashenko, P. Piskorz, I. Komaromi, R. Gomperts, R.L. Martin, D.J. Fox, T. Keith, M.A. Al-Laham, C.Y. Peng, A. Nanayakkara, C. Gonzalez, M. Challacombe, P.M.W. Gill, B. Johnson, W. Chen, M.W. Wong, J.L. Andres, C. Gonzalez, M. Head-Gordon, E.S. Replogle, J.A. Pople, Gaussian 98, Revision A.7, Gaussian, Inc., Pittsburgh, PA, 1998.
[24] T.H. Dunning, III, P.J. Hay, in: H.F. Schaeferiii (Ed.), Modern Theoretical Chemistry, Plenum Press, New York 1976, p. 1.
[25] (a) P.J. Hay, W.R. Wadt, J. Chem. Phys. 82 (1985) 270;
(b) W.R. Wadt, P.J. Hay, J. Chem. Phys. 82 (1985) 284;
(c) P.J. Hay, W.R. Wadt, J. Chem. Phys. 82 (1985) 299.
[26] S.E. Boyd, L.D. Field, T.W. Hambley, M.G. Partridge, Organometallics 12 (1993) 1720.